Journal of Imaging Science and Technology® 51(3): 217–224, 2007.

Design of Novel Reducing Agents for Direct Thermographic Materials

Leif P. Olson
University of Rochester Medical Center, Rochester, New York 14642
E-mail: leif_olson@URMC.rochester.edu

Peter J. Cowdery-Corvan
Eastman Kodak Company, 1999 Lake Avenue, Rochester, New York 14650-2112

David R. Whitcomb and Kumars Sakizadeh
Eastman Kodak Company, 1 Imation Way, Oakdale, Minnesota 55128

Louis M. Leichter
Mendota Heights, Minnesota 55120

Abstract. *We describe the systematic design and evaluation of new phenolic reducing agents (developers) for dry-processed, silver-based direct thermographic (TG) black-and-white films for medical diagnostic imaging. In TG media, heat exposure as short as 7 ms/pixel is used to induce development, thus highly active developers are needed. Our approach to this problem combined synthesis, coating evaluation, and electronic structure calculations to provide insights into the TG development mechanism. The computed highest occupied molecular orbital (HOMO) energy of the neutral developer did not correlate with maximum image density (D_{max}). Rather, the best developers (high D_{max}, low fog) had relatively low phenol O-H deprotonation energies and high-lying phenolate anion HOMO energies, implying that, in the TG process, silver is reduced primarily by phenolate ion. This information allowed discovery of new categories of potentially useful TG developers, including ortho-aminophenol, para-aminophenol, halophenol, and resorcinol derivatives.* © *2007 Society for Imaging Science and Technology.*
[DOI: 10.2352/J.ImagingSci.Technol.(2007)51:3(217)]

INTRODUCTION

Directly imaged silver-carboxylate-based black-and-white thermographic (TG) films are compositionally simpler than related photothermographic (PTG) films.[1,2] TG media fundamentally require only a silver source (usually silver salts of long chain fatty acids), a developer (i.e., reducing agent), a toner (an auxiliary agent that influences development activity as well as modifying the hue of the image), a binder (usually a polymer such as polyvinylbutyral, e.g., Butvar), and a support. Application of heat in an imagewise fashion provides an image from the formation of metallic silver nanoparticles:

$$\mathrm{Ag(O_2CC}_n\mathrm{H}_{2n+1}) + \text{Toner} + \text{Developer} + \text{heat} \rightarrow \mathrm{Ag^0} + \text{Toner} + \text{Oxidized Developer} + \mathrm{HO_2CC}_n\mathrm{H}_{2n+1}. \quad (1)$$

Received Oct. 2, 2006; accepted for publication Dec. 19, 2006.
1062-3701/2007/51(3)/217/8/$20.00.

All of these components are also present in PTG materials, which additionally contain light-sensitive components and related auxiliary agents that are absent in TG materials.[1] However, important kinetic differences exist in the two imaging processes. The PTG system is usually processed by 15 sec of heating at 122°C.[1] This is done in a "nonimagewise" fashion, i.e., all regions of the image are heated equally; the density variations that form the image correlate to light exposure, not local variations in thermal heating. The TG material, on the other hand, lacks light-sensitive components. It is imaged by a moving thermal printhead that is imagewise heated where the heating correlates with the desired density of a pixel. Thermal dwell times for TG materials are typically 7–17 ms/pixel with the printhead having a surface temperature in the 300–400°C range,[2] yielding an in-film maximum temperature that can be estimated from correlation of x-ray data with the silver soap thermal phase transitions[3] to be about 170°C. Most importantly, this means the TG film experiences a higher temperature than a PTG film, but for a time that is about 1000–2000 times shorter.

Because of the difference in process times between PTG and TG systems, imaging components that function very effectively in a PTG film may not function well (or at all) in a TG film or vice versa. New or different components are needed. Among these, it is of crucial importance to incorporate developers that are effective in the TG process. Discovery of such developers was the main goal of the present work, with an effort to broaden the scope of chemical structures beyond catechol (1,2-dihydroxybenzene) and hydroquinone (1,4-dihydroxybenzene), some of which are known to be effective TG developers[4] and, as has been known for many decades, hydroquinone and derivatives are reducing agents useful in conventionally processed black-and-white photographic media.[5] Despite our interest in novel structures, some structure restrictions were required for practical

reasons; hence we chose the scope of the current study to structures containing one or more aryl-OH groups. Although primarily intended as an effort to discover new and more useful materials, it was thought that the interplay between theory and experiment would reveal mechanistic features of the redox reaction between a silver salt and phenolic reducing agent under fast, hot TG processing conditions that differ substantially from the reaction mechanism[6] that occurs with slower, milder PTG processing conditions. We report here the successful approach that was used to find active, novel TG[7] developers among aminophenol, halophenol, and even resorcinol derivatives that are useful in the imaging formulations.

EXPERIMENTAL

Computational Methods

Prediction of favored molecular conformations and tautomers was done using the approximate PM3 semiempirical quantum mechanics method.[8,9] The PM3-predicted low-energy structures were refined using the B3LYP "hybrid" density functional theory method,[10] using the 6−31G* basis set.[11]. For molecules containing elements for which the 6−31G* basis set is not available, a very similar B3LYP/LACVP* method was used instead.[12–14] This method places the 6−31G* basis set on all available atoms in the molecule for which it is available, but the effective core potential LACVP basis set is placed on the remaining atoms (e.g., bromine). The procedure used to determine the deprotonation energies and anion highest occupied molecular orbital (HOMO) energies of the reducing agents involved the following steps.

(A) The lowest-energy conformation of the reducing agent, in its deprotonated form and its nondeprotonated form, was predicted at the HF/PM3 level. Among the most important features varied were the intramolecular hydrogen bonds, if any. Also, if there was more than one ionizable proton in the structure, it was necessary to evaluate the relative energies of isomeric structures bearing the same molecular charge and with varied positions of the protons (e.g., tautomers). This was done using an automated systematic conformational search procedure implemented in Spartan '02.[15,16]

(B) The lowest energy structures from Step A (deprotonated and nondeprotonated phenols) were refined by gas-phase geometry optimization at the B3LYP/6−31G* (or B3LYP/LACVP*, if necessary) level using Jaguar, version 4.1 or 5.0.[17]

(C) Single-point B3LYP/6−31G* solvation calculations were performed using step (B) geometries of the deprotonated and nondeprotonated phenols. The self-consistent reaction field model[18] implemented in Jaguar was used. Melts of the highly hydrolyzed polyvinylbutyral binder containing other components of the coating have an overall dielectric constant (ε) of about 21, similar to ethanol or acetone. Nonetheless the solvent chosen was water ($\varepsilon = 78.5$), for the following reasons: (a) It is unknown what ε may be within the TG imaging layer (especially during actual thermal processing); (b) the coating is heterogeneous, so it might contain highly polar microenvironments (e.g., in the vicinity of silver salts) possibly making an average ε value misleading; (c) in case the quality of parametrization (i.e., with respect to experimental data) of solvation models is not equal for all solvents, it seemed likely that water would be better parametrized than organic solvents for ionic species; (d) in the statistical approach used here it is not important to reproduce absolute solvation energies (only the trend is important); and (e) at early stages of this work, it seemed likely that we might eventually desire to correlate computed deprotonation energies with experimental (aqueous) pK_a values.

(D) The results of the step (C) solvation calculations were evaluated to obtain values of interest. The values used were the gas-phase energy, the solution-phase energy (defined as the sum of the total solute energy, total solvent energy, solute cavity energy, and first-shell correction factor), and the solution-phase HOMO energies of the deprotonated and nondeprotonated reducing agents. From this, three key "descriptors" (akin to descriptors used in quantitative structure-activity relationship studies) were determined. The first descriptor is "Deprot_{aq}", i.e., the aqueous deprotonation energy, or the difference between the solution-phase energies of the nondeprotonated and deprotonated reducing agent in units of kcal/mol. This is a correlate of a pK_a value. The computed energy differences for various phenol $\rightarrow$ phenolate deprotonation reactions are for half-reactions, therefore the absolute values of the computed energies are very large, ca. 300 kcal/mol (about 13 eV). (For a properly balanced chemical reaction, one could subtract Deprot_{aq} of some appropriate standard, e.g., Deprot_{aq} for C_6H_5OH = 305.9 kcal/mol, thus making the absolute values smaller.) The second descriptor is "Gas versus Aq," which is simply the difference between "Deprot_{gas}" (the gas-phase deprotonation energy) and Deprot_{aq}; the intent is to provide a computed value that reflects how the molecular structure influences solvent participation in the deprotonation step. The third descriptor is the "anion HOMO," i.e., the HOMO energy of the deprotonated reducing agent, in eV, taken directly from the solvation calculation, a correlate of the oxidation potential.

The computed descriptors were used to evaluate potential reducing agents and were also used in a limited statistical analysis, with respect to D_{max} of the 17 different reducing agents, shown in Table I for the structure based on Figure 1. Statistical analysis was performed using JMP 5.0.[19]

Synthesis

All compounds were either obtained commercially or prepared by standard synthetic procedures. An example of the resorcinol preparation is given below, Figure 2.

(1) The intermediate ester was made using a slightly adapted literature procedure.[20] Ten g of acid was refluxed in 100 ml of BF_3/methanol complex (12%, in excess methanol) for four days. The solvent was removed; the residue was dissolved in toluene and washed with $NaHCO_3$ (10%) until

Table I. Structures of potential reducing agents evaluated.

Compound	X1	X2	X3	X4	X5
RA-1	NH_2	H	COOH	H	H
RA-2	NH_2	H	H	COOH	H
RA-3	NH_2	H	CF_3	H	H
RA-4	NH_2	H	H	$COOCH_3$	H
RA-5	NH_2	H	CN	H	H
RA-6	NH_2	H	$COOCH_3$	H	H
RA-7	NH_2	H	NO_2	H	H
RA-8	NH_2	H	SO_2CH_3	H	H
RA-9	NH_2	H	H	SO_2CH_3	H
RA-10	Cl	H	NH_2	H	Cl
RA-11	H	COOH	NH_2	H	H
RA-12	COOH	H	OH	H	H
RA-13	Br	H	OH	H	H
RA-14	Cl	H	OH	H	H
RA-15	Cl	H	OH	Cl	H
RA-16	Cl	Cl	OH	Cl	Cl
RA-17	$C(=O)NHCH_3$	H	OH	H	H

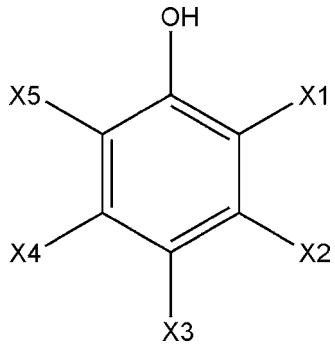

Figure 1. Generic structure of evaluated phenolic reducing agents.

gas evolution stopped, then washed with water. The toluene solution was dried with $MgSO_4$, filtered, and evaporated to a solid.

(2) The N-methylamide was made by dissolving 2 g of the ester in 10 mL of 40% methylamine in water. After stirring overnight, the mixture was concentrated, then acidified with 1 N HCl, which precipitated the amide. The solid sample was collected by filtration, washed, and dried under vacuum (m.p.=187°C compared to the literature value of 191°C).[21]

Preparation of Thermographic Coatings

Details of the preparation of the formulations used for thermographic imaging evaluations are given elsewhere.[22] Generally, the films were prepared by coating silver behenate, 2,3-dihydroxybenzoic acid (23DHB), phthalazinone (PAZ), or benzoxazinedione (BOD), Figure 3, at approximately 50 and 25 mol % relative to the silver behenate, in an MEK solution of binder (Monsanto Butvar B-79). A protective topcoat was added based on cellulose acetate (CAB-171-15S, Eastman Chemicals). The resulting thermographic films were imaged with an Agfa DryStar 2000 printer with a standard test pattern.

RESULTS AND DISCUSSION

The approach taken to design and evaluate new developers for TG imaging materials was to combine synthesis and coating evaluation with mechanistic investigation. Much of this work involved use of first-principles calculation methods (density functional theory) to evaluate developer structures, compute various properties in a search to find those related to the developer reaction mechanism, and design new developers based on these calculations prior to synthesis and evaluation. At the outset, we hypothesized that the HOMO energy of the neutral phenol (an easily computed quantity and usually not highly dependent upon molecular conformation or environment) would be a reasonable predictor of TG activity and, hence, correlate with D_{max}. This proved not to be true; therefore the computational methods described here are the result of a trial and error process. We screened numerous candidate phenols computationally. Each of these had to be optimized in at least two protonation states, namely neutral phenol and anionic phenolate, but sometimes several tautomers of each neutral and/or ionic structure had to be optimized. Most phenols had more than one possible conformation, so the lowest energy conformation had to be identified. Corrections were made for solvent effects given that gas-phase energies, especially of ionized species, can sometimes be misleading. Although the immediate concern of our research is finding new materials, a mechanistic understanding was also desired. As such, these results complement ongoing studies of TG mechanisms, such as those involving surface enhanced Raman spectroscopy and electron microscopy.[23,24] Some useful mechanistic generalizations can be made based on the present work. As will be shown, the best TG phenolic reducing agents tend to have a combination of a relatively low computed deprotonation energy (correlating with low pK_a) and a relatively high-lying anion HOMO energy (the phenolate ion is easily oxidized). This result points toward the phenolate as the active reducing species, yet the results also indicate that, once they are formed, some phenolates will more readily reduce silver than others. This presented a design challenge, inasmuch as structural features that favor phenol deprotonation (e.g., electron-withdrawing groups) generally make the resulting phenolate ion resistant to oxidation. However, non-catechol reducing agents were found among *ortho*-aminophenol, *para*-aminophenol, resorcinol, and hydroquinone derivatives.

Mechanistic Overview

Three separate lines of evidence support our hypothesis that even in the dry TG format, phenolic reducing agents do not substantially react as the neutral phenol. The first is that substituted catechols such as 3,4-dihydroxybenzonitrile (34DHBN)[25] and 3,4-dihydroxybenzophenone (34DHBA),[26]

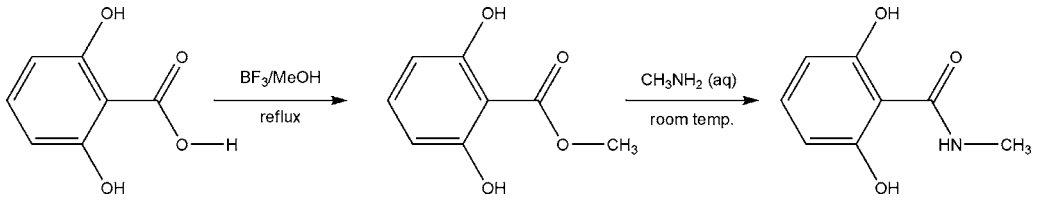

Figure 2. γ-Resorcylamide preparation procedure.

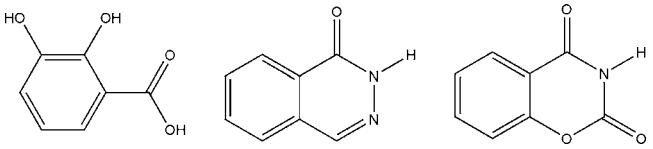

Figure 3. Structures for 23DHB, PAZ, and BOD.

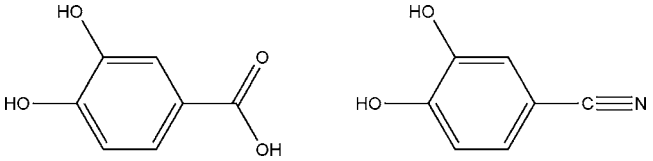

Figure 4. Known thermographic developers.

Figure 4, are known in the imaging literature as active TG developers.

One may ask why 34DHBN (for example) is an active TG developer. If the mechanism is simple electron transfer from the neutral phenol to Ag^+ to yield a developer radical cation, then the presence of a cyano group is quite the opposite of what would be expected. Electron-withdrawing groups such as cyano (Hammett σ value for *p*-cyano group=0.66[27]) should significantly destabilize the radical cation. Electron withdrawal will, however, favor deprotonation of the phenol hydroxy groups (most notably the 4-hydroxy group). An additional driving force that aids deprotonation of catechols is provided by the *ortho* orientation of the two hydroxy groups, which allow intramolecular hydrogen bonding that stabilizes the phenolate anion. Phenolates are much stronger reducing agents than phenols, and formation of the anion should increase reducing power sufficiently to outweigh electron-withdrawing effects of groups like cyano.

A second line of evidence against the idea of reaction from the neutral phenol in the TG media is that reducing agents of the bisphenol type used in PTG media are virtually inactive in TG media.[1] Mechanistic studies show that the bisphenol silver reduction mechanism involves initial loss of an electron from the developer, such as shown in Figure 5, in the slower-processed PTG format. This is not at all surprising, considering that each aryl ring bears four electron-donating substituents, which would substantially stabilize the radical cation.[28–30] Such substituents will tend, however, to destabilize the phenolate form (even though hydrogen bonding between the phenols partly counteracts this effect).

An additional point about bisphenol developers is that extracts of exposed and processed PTG films reveal significant amounts of 2, 4, 6, 8, 10, and 12-electron oxidized developers.[29] It is reasonable to suggest that the formation of up to 12-electron oxidized developers can occur effectively only in the relatively long timeframe of the PTG process. That is, the weak TG silver-reducing performance of bisphenols may be related to their building up image density in PTG films by the cumulative effect of a series of consecutive silver-reducing reactions that require seconds of heating; but this extensive series of reactions does not occur in the milliseconds development times used in TG media.

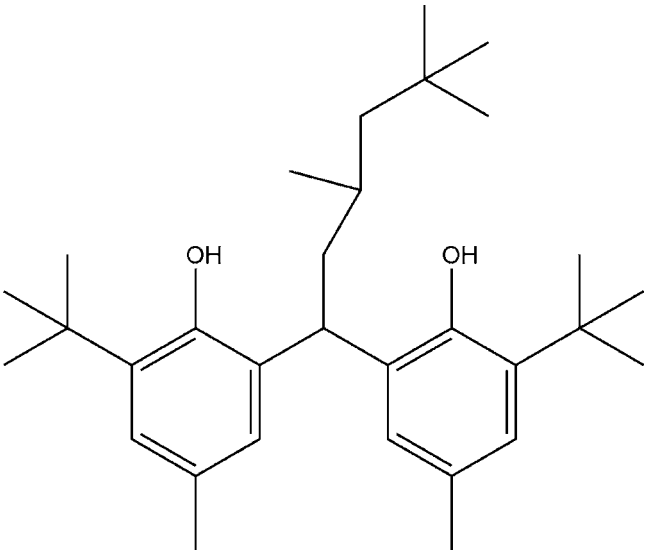

Figure 5. Typical PTG bisphenol developer.

A third line of evidence that supports our mechanistic hypothesis is found in the present study, i.e., a limited statistical analysis that compares our computed descriptors to experimentally determined D_{max} values (i.e., raw density, not corrected for D_{min}—the density in the nonimage area, which was quite variable) for a set of 17 phenolic reducing agents in a TG formulation. Testing various least-squares fits with JMP 5.0, the computed parameters used were neutral HOMO, $Deprot_{aq}$, $Deprot_{gas}$, anion HOMO, and the difference between $Deprot_{gas}$ and $Deprot_{aq}$ (Gas versus Aq). After running all possible models that included 1–5 parameters, no model was found where the neutral HOMO energy was a significant predictor for D_{max}. $Deprot_{aq}$ showed more predictive ability than $Deprot_{gas}$. The anion HOMO energy was significant, but only if $Deprot_{aq}$ (or $Deprot_{gas}$) was included in the model. Finally, Gas versus Aq was statistically significant, but less so than either $Deprot_{aq}$ or anion HOMO.

Using this information, it was possible to construct a mechanistic picture, also used subsequently as a guideline

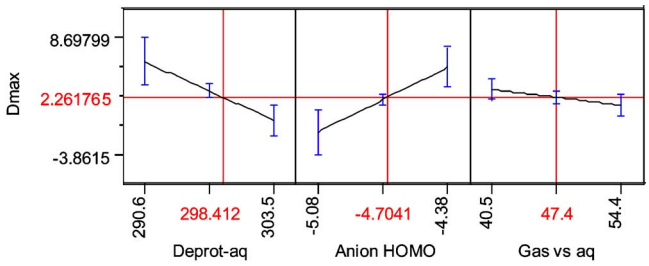

Figure 6. JMP leverage plots of D_{max} vs computed descriptors. Dotted lines represent the median values of the data, with mean values listed near the center of the individual axes. The slopes of the solid lines (depicted with error bars) show whether a given predictor has a negative or positive influence on D_{max}, as well as its importance relative to the other predictors.

for design of novel developers. The proposed mechanism is a consequence of the statistical significance of the computed parameters (1) $Deprot_{aq}$, (2) anion HOMO, and (3) Gas versus Aq. This last parameter was thought to be a measure of how much solvent reorganization is involved in ionization of the phenol; the underlying reasoning here is that if a relatively large amount of participation from the "solvent" (e.g., the Butvar binder plus any other neighboring materials in the coating) is required, the ionization process may proceed less efficiently. Butvar-type polymeric binders have been proposed to actively participate in the thermal reduction reaction of direct thermal imaging materials by their capability to reduce silver behenate directly.[31]

Least-squares analysis with these three predictors yields a model with $R^2=0.608$. That the model is imperfect is to be expected, given the numerous assumptions, only one of which is the inherent shortcomings of computational models. Likely of greatest importance is that solubility problems can sometimes cause anomalously low D_{max} values, as undesired crystallization might occur in the coating, even if the developer dissolves adequately in the melt. An improved fit might be obtained with more complex models (e.g., inclusion of cross terms), however this was not done inasmuch as it was thought that this would add little if any interpretive value. In any case, our three key descriptors are shown to be statistically significant, with the two "main" descriptors ($Deprot_{aq}$ and anion HOMO) being highly statistically significant, Figure 6.

The $Deprot_{aq}$ and anion HOMO parameters are highly statistically significant ($p<0.006$ and $p<0.004$). For the Gas versus Aq parameter, $p<0.093$, statistical significance is less certain. Inspection of the JMP leverage plots, Fig. 6, reveals that the TG D_{max} tends to respond favorably to phenols with

- Low $Deprot_{aq}$ (correlates with a low pK_a).
- Relatively less negative anion HOMO (easily oxidized phenolate anion).
- Low Gas versus Aq value (implying relatively little solvation assistance of the ionization process. Hydrogen bond donating groups *ortho* to the phenolate oxygen seem associated with a low value for this parameter).

This is consistent with a development mechanism that involves deprotonation of the phenol as the first step, and electron transfer as a second step (although we discuss this as a two-step process, it is also conceivable that a concerted deprotonation/electron-transfer mechanism occurs, if the HOMO of such a transition state correlates with the anion HOMO). It is inconsistent with direct oxidation of the neutral phenol to yield a radical cation. It also fits with the high TG activity of relatively electron-deficient compounds like 34DHBN, the low TG activity of electron-rich developers (including those of the PTG bisphenol type), and the observation that the neutral HOMO did not correlate with TG D_{max}.

Perhaps noteworthy is the finding that the anion HOMO is important. One could have reasonably hypothesized that at the high temperatures used in TG imaging, the reaction between silver ion and phenolate ion would be too facile to significantly influence density, thus only the deprotonation energy should be important; but that hypothesis is incorrect. The design challenge was to translate these characteristics into novel structures, with a particular problem being that the same substituents that are right-way for phenol ionization are generally wrong-way for phenolate anion redox activity.

Classes of useful phenols

Comparing initial screening results and calculated parameters led to the identification of several new classes of active developers. Without describing all of the developers that were screened computationally and experimentally, the compounds that were identified as yielding useful D_{max} levels tended to fall into the following classes:

a. *ortho*-aminophenols, resorcinols, and their amido and sulfonamido derivatives;
b. *para*-aminophenols and amido and sulfonamido derivatives; and
c. hydroquinones, particularly bearing electron-withdrawing groups.

In some cases, it was noted that one or more chlorine or bromine atoms on the aryl ring could advantageously lower the deprotonation energy without much of an adverse impact on the anion HOMO energy. This chloro/bromo effect was particularly apparent in the case of hydroquinones, but it might be a more general phenomenon.

A potential advantage of *ortho*-aminophenols (including derivatives such as amides and sulfonamides) compared to the nominally isoelectronic catechol moiety is design flexibility. For example, replacement of one of the catechol OH groups with NHR allows the molecule to maintain an intramolecular hydrogen bond that favorably influences the phenol ionization, but in a tunable way by varying the substituent R. It was found that electron-withdrawing R groups on NHR (e.g., R=carbonyl) promote a strong NH···O hydrogen bond (as shown by relatively long N-H distances and relatively short H-O distances) that tends to lower the phenol deprotonation energy. Conversely, electron-releasing R groups have less beneficial deprotonation energy effect but

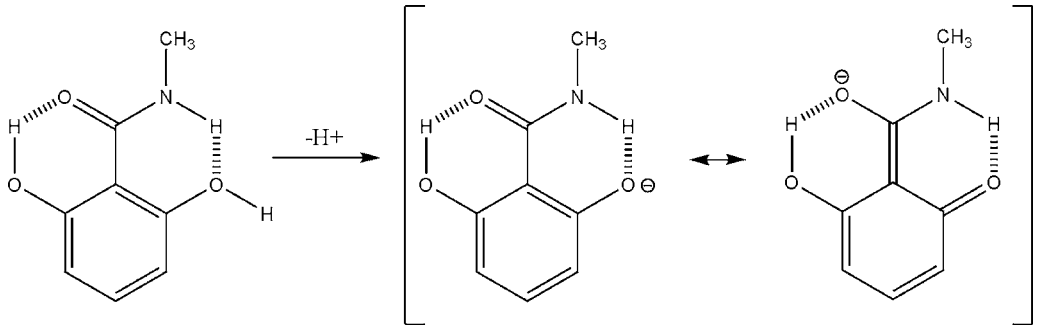

Figure 7. γ-Resorcylamide deprotonation equilibria.

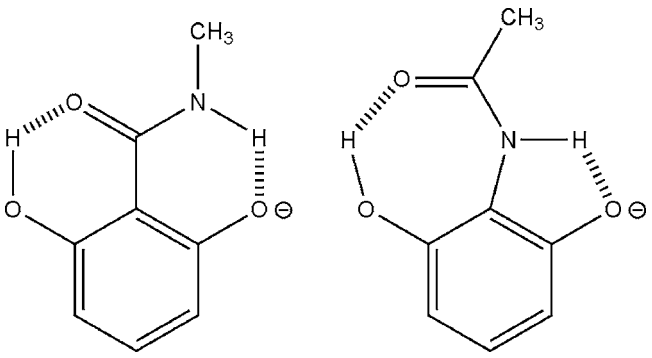

Figure 8. Anion hydrogen bonding pattern for γ-resorcylamide (left: $Deprot_{aq}$ = 298 kcal/mol; anion HOMO −4.85 eV) and the "reverse amide" structure (right: $Deprot_{aq}$ = 300 kcal/mol; anion HOMO = −4.55 eV). The internal hydrogen bonding of the reverse amide is sufficiently stabilizing to permit a reasonably low $Deprot_{aq}$ value while at the same time yielding a desirable anion HOMO energy.

can (desirably) raise the anion HOMO energy. Some tuning is also possible for *para*-aminophenol derivatives, although in this case the effect is through resonance and induction effects rather than hydrogen bonding to the phenol moiety.

Typically, resorcinols (1,3-dihydroxybenzenes) do not function well as developers because they are not as electron-rich as 1,2- or 1,4-dihydroxybenzenes, and their pK_as, while lower than 1,4-dihydroxybenzene, is not as low as 1,2-dihydroxybenzene. Certain resorcinol derivatives, however, can produce a hydrogen-bonded stabilized anion. For example, the computed deprotonation energy of the amide shown in Figure 7 is only ~298 kcal/mol, and the anion HOMO is about −4.85 eV. These numbers are within a range observed for the active developers described above.

Active developers may also be obtained from the structural variation of γ-resorcylamide as in the so-called "reverse amide" structure, Figure 8. We calculated the deprotonation energy and anion HOMO energies to compare to the γ-resorcylamide. Comparing the calculated results for the two isomers, it appears that the reverse amide deprotonation is only ~2 kcal/mol less favorable than the γ-resorcylamide. Meanwhile the anion HOMO has moved in a distinctly favorable direction, +0.3 eV. Considering these results, we would suggest that the reverse amide class is worthy of consideration as reducing agents.

Table II lists comparative compounds C-1 to C-7 that, in contrast to the compounds listed in Table I, were generally found to have unacceptable reactivity. We attribute this result to relatively high $Deprot_{aq}$ energies, as the neutral and anion HOMO energies were generally relatively favorable.

Table II. Structures of comparative developer compounds.

Compound	X1	X2	X3	X4	X5
C-1	NH_2	H	H	H	H
C-2	NH_2	H	OCH_3	H	H
C-3	H	H	NH_2	H	H
C-4	H	OCH_3	NH_2	H	H
C-5	OCH_3	H	NH_2	H	H
C-6	H	H	OH	H	H
C-7	OCH_3	H	OH	H	H

An example that illustrates the results with these phenols (RA-1) to (RA-17) and (C-1) to (C-7) is given in the following section. The results summarized in Table III demonstrate the following.

Ortho-aminophenol compounds having an aqueous deprotonation energy of less than 307 kcal/mol and preferably less than 305 kcal/mol, along with an anion HOMO energy more negative than −4.17 eV and preferably more negative than −4.34 eV, provided thermographic materials with low D_{min} and high D_{max}. A comparative thermographic material incorporating the parent compound, *ortho*-aminophenol (sample 1-1, compound C-1) had an unacceptably high D_{min}. Comparative compound C-2, which has an electron-releasing group on the benzene ring, would be expected to behave similarly to the *ortho*-aminophenol.

Para-aminophenol compounds having an aqueous deprotonation energy of less than 310 kcal/mol, and preferably less than 309 kcal/mol, along with an anion HOMO energy more negative than −4.18 eV provided thermographic materials with low D_{min} and high D_{max}. A comparative thermographic material incorporating the parent compound, *para*-aminophenol (sample 1-12, compound C-3) had an unacceptably high D_{min}. Comparative compounds C-4 and C-5 that have electron-releasing groups on the benzene ring would be expected to behave similarly to the *para*-aminophenol.

Table III. Calculated developer parameters correlation to D_{min} and D_{max}.

Sample	Compound	D_{min}	D_{max}	Aqueous Deprotonation Energy—kcal/mol (eV)	Anion HOMO Energy—(eV)
ortho-Amino phenols					
1-1	C-1	0.39	2.77	307 (13.3)	–4.13
1-2	C-2	—	—	308 (13.3)	–4.17
1-3	RA-1	0.18	2.33	298 (12.9)	–4.61
1-4	RA-2	0.20	3.82	305 (13.2)	–4.37
1-5	RA-3	0.17	2.64	301 (13.0)	–4.53
1-6	RA-4	0.17	2.50	306 (13.3)	–4.34
1-7	RA-5	0.17	3.09	298 (12.9)	–4.63
1-8	RA-6	0.25	2.80	299 (13.0)	–4.53
1-9	RA-7	0.24	4.29	294 (12.7)	–4.78
1-10	RA-8	0.25	2.64	298 (12.9)	–4.69
1-11	RA-9	0.24	2.31	302 (13.1)	–4.52
para-Amino phenols					
1-12	C-3	0.44	2.57	313 (13.6)	–3.62
1-13	C-4	—	—	310 (13.4)	–4.33
1-14	C-5	—	—	312 (13.5)	–4.26
1-15	RA-10	0.22	2.21	297 (12.9)	–4.44
1-16	RA-11	0.19	0.37	309 (13.4)	–4.18
Hydroquinones					
1-17	C-6	0.17	1.52	311 (13.5)	–4.06
1-18	C-7	—	—	311 (13.5)	–4.04
1-19	RA-12	0.22	3.12	294 (12.7)	–4.93
1-20	RA-13	0.26	3.47	302 (13.1)	–4.43
1-21	RA-14	0.25	3.36	303 (13.1)	–4.38
1-22	RA-15	0.26	3.71	299 (13.0)	–4.70
1-23	RA-16	0.28	3.82	293 (12.7)	–4.86
1-24	RA-17	0.25	2.98	303 (13.1)	–4.54

Hydroquinones having an aqueous deprotonation energy of less than 311 kcal/mol and preferably less than 303 kcal/mol along with an anion HOMO energy more negative than −4.06 eV, and preferably more negative than −4.28 eV, provided thermographic materials with low D_{min} and high D_{max}. A comparative thermographic material incorporating the parent compound, hydroquinone (sample 1-17, compound C-6), had an unacceptably low D_{max}. Comparative compound C-7, which has an electron-releasing group on the benzene ring, would be expected to behave similarly to hydroquinone.

CONCLUSIONS

This work demonstrates how theory, synthesis, and evaluation can work together to make progress in an important, practical materials science application; in this case, design of active incorporated reducing agents for direct thermographic materials based on the thermal reduction of silver carboxylates. While the short term goal of the present work is discovery of new materials for immediate practical needs, there is also a long-term mechanistic component as a foundation for designing subsequent generations of reducing agents or other components that interact with the silver reduction process. It is important to emphasize that this same approach may be directly applicable to other thermographic imaging materials, such as PTG films, where more efficient imaging initiated by a designed developer decreases the amount of silver required in the formulation.

The emerging mechanistic picture that seems to characterize the current TG imaging format is that phenolic developers prefer to reduce the silver ion via their phenolate form. This led to a design challenge to find substitution patterns that would lower the phenol deprotonation energy but without strongly deactivating the resulting phenolate ion toward oxidation. Despite this constraint, active developers have been found among *ortho*-aminophenols, *para*-aminophenols, resorcinols, hydroquinones, and derivatives of these, for example, amidophenols and chlorohydroquinones.

REFERENCES

[1] P. J. Cowdery-Corvan and D. R. Whitcomb, *Handbook of Imaging Materials*, edited by A. S. Diamond and D. S. Weiss (Marcel Dekker,

New York, 2002), p. 473.
[2] M. de Clerck, *Proc. ICPS '98 Int. Conf. Imaging. Sci.* (KVCV, Antwerp, Belgium, 1998) p. 106.
[3] I. Geuens, H. Hoogmartens, and G. Defieuw, US Patent 6,677,274 (2004).
[4] P. Dooms, I. Hoogmartens, and G. Defieuw, US Patent 6,693,062 (2004).
[5] A. Lumière, L. Lumière, and A. Seyewetz, Brit. J. Photog. **61**, 341 (1914).
[6] T. Maekawa, M. Yoshikane, H. Fujimura, and I. Toya, J. Imaging Sci. Technol. **45**, 365 (2001).
[7] L. P. Olson, D. R. Whitcomb, P. J. Cowdery-Corvan, K. Sakizadeh, T. Ishida, and L. M. Leichter, Direct Thermographic Materials with Phenolic Reducing Agents, US Patent 7,135,432 (2006).
[8] J. J. P. Stewart, J. Comput. Chem. **10**, 209 (1989).
[9] J. J. P. Stewart, J. Comput. Chem. **10**, 221 (1989).
[10] A. D. Becke, J. Chem. Phys. **98**, 5648 (1993).
[11] P. C. Hariharan and J. A. Pople, Theor. Chim. Acta **28**, 213 (1973).
[12] P. J. Hay and W. R. Wadt, J. Chem. Phys. **82**, 270 (1985).
[13] W. R. Wadt and P. J. Hay, J. Chem. Phys. **82**, 284 (1985).
[14] P. J. Hay and W. R. Wadt, J. Chem. Phys. **82**, 299 (1995).
[15] Wavefunction, Inc., 18401 Von Karman Avenue, Suite 370, Irvine, CA 92612; www.wavefun.com
[16] *Spartan '02 Linux/Unix Tutorial and User's Guide* (Wavefunction, Inc., Irvine, CA, 2001), pp. 215–217.
[17] Schrödinger, Inc., Portland, OR.
[18] B. Marten, K. Kim, C. Cortis, R. A. Friesner, R. B. Murphy, M. N. Ringnalda, D. Sitkoff, and B. Honig, J. Phys. Chem. **100**, 11775 (1996).
[19] JMP, Release 5.0, SAS Institute, Inc., Cary, NC, 2002.
[20] A. Mendel, Organic Preparations and Procedures **2**, 295 (1970).
[21] K. Tomino, Yakugaku Zasshi **78**, 1425 (1958).
[22] S. Chen, B. Stwertka, P. Cowdery-Corvan, D. R. Whitcomb, and L. Burleva, J. Imaging Sci. Technol. **51**, 225 (2007).
[23] D. R. Whitcomb, M. Rajeswaran, S. Chen, and P. Cowdery-Corvan, *Proc. ICIS '06, International Conference of Imaging Sciences* (IS&T, Springfield, VA, 2006) p. 218.
[24] S. Chen, B. Stwertka, P. Cowdery-Corvan, D. R. Whitcomb, and L. Burleva, *ibid.*, p. 211.
[25] P. Dooms, I. Hoogmartens, and G. Defieuw, EP 1270255 (2003).
[26] T. M. Conder and K. P. O'Leary, US Patent 4,082,879 (1978).
[27] C. Hansch, A. Leo, and R. Taft, Chem. Rev. (Washington, D.C.) **91**, 165 (1991).
[28] H. Akahori, K. Morita, A. Nishijima, T. Mitsuhashi, K. Ohkubo, and S. Fukuzumi, *Proc. ICPS '02 International Conference Imaging Science* (SPSTJ, Tokyo, Japan, 2002), p. 35.
[29] H. Akahori, K. Morita, A. Nishijima, T. Mitsuhashi, K. Ohkubo, and S. Fukuzumi, J. Imaging Sci. Technol. **47**, 124 (2003).
[30] H. Akahori, K. Morita, A. Nishijima, T. Mitsuhashi, K. Ohkubo, and S. Fukuzumi, J. Imaging Sci. Technol. **49**, 381 (2005).
[31] F. Ruttens, J. Imaging Sci. Technol. **43**, 545 (1999).